Int. J. Electron. Commun. (AEÜ) xxx (2013) xxx–xxx

Contents lists available at SciVerse ScienceDirect

International Journal of Electronics and Communications (AEÜ)

journal homepage: www.elsevier.com/locate/aeue

A tuned rectifier for RF energy harvesting from ambient radiations

Gaurav Singh [a], Rahul Ponnaganti [a], T.V. Prabhakar [a,*], K.J. Vinoy [b]

[a] Department of Electronic Systems Engineering, Indian Institute of Science, Bangalore, India
[b] Electrical Communication Engineering, Indian Institute of Science, Bangalore, India

ARTICLE INFO

Article history:
Received 17 September 2012
Accepted 15 December 2012

Keywords:
Cell-tower radiations
RF energy harvesting
Tuned rectifier
Supercapacitor

ABSTRACT

A circuit topology based on accumulate-and-use philosophy has been developed to harvest RF energy from ambient radiations such as those from cellular towers. Main functional units of this system are antenna, tuned rectifier, supercapacitor, a gated boost converter and the necessary power management circuits. Various RF aspects of the design philosophy for maximizing the conversion efficiency at an input power level of 15 μW are presented here. The system is characterized in an anechoic chamber and it has been established that this topology can harvest RF power densities as low as 180 μW/m^2 and can adaptively operate the load depending on the incident radiation levels. The output of this system can be easily configured at a desired voltage in the range 2.2–4.5 V. A practical CMOS load – a low power wireless radio module has been demonstrated to operate intermittently by this approach. This topology can be easily modified for driving other practical loads, from harvested RF energy at different frequencies and power levels.

1. Introduction

A wirelessly powered wireless terminal has been the dream of many researchers for at least a decade [1]. With the wide proliferation of wireless technologies energy transmitted by broadcast stations, cellular base stations and Wi–Fi access points is available for potential use to operate low power electronic devices. One such experiment conducted at Intel labs, reports harvesting about 60 μW of power from television (TV) broadcasting tower [2]. Energy harvesting from electromagnetic sources is typically accomplished by having a rectifier circuit connected to a receiver antenna, which converts microwave energy into DC. One of the key performance measures of these rectifiers is their RF to DC conversion efficiency. Conversion efficiencies up to 80% has been reported for wireless power transmission (WPT) at various microwave frequencies [3–7], but those used in an energy harvesting system are somewhat different from WPT as the power levels associated with the latter are typically three orders of magnitude lower. Power levels available from a typical cellular base station with a rating of 20 W and 17 dbi directional gain is about 320 μW/m^2 at a distance of 500 m [8]. Assuming a standard dipole antenna of gain 2.14 dB the received power at input power density of 320 μW/m^2 is only 4 μW, which is insufficient to drive low power devices.

When scavenging energy at such low power densities another parameter which is of practical interest is the output DC voltage available. Voltages of about 2 V, with RF–DC conversion efficiency >20% have been reported at received power levels of 10 μW, but these are very sensitive to the load impedances and are obtained only when very high impedances (>5 MΩ) are connected. The output voltage and efficiency drops to about 100 mV and 1% respectively, when the load impedance is reduced to 0.33 MΩ [9]. Another reported circuit topology combines the output from multiple rectifier circuits cascaded or cascoded to form a series or parallel combination to increase the voltage or the current, respectively [10]. However the use of multiple rectifiers would occupy large area as each of these would require a separate antenna. Alternatively, DC–DC boost converters may be used along with rectifiers to generate sufficient output voltage and current. Commercially available DC–DC boost converters can boost input voltages as low as 20 mV, but have an input power requirement of about 63–80 μW [11,12], which is much higher than the 4 μW available input power. Another limitation is that when connected as load the boost converter offers a very low resistance of less than 6Ω [12], whereas the desirable impedance as discussed earlier is higher. A commercial product from PowerCast is also available which uses boost converter and works at received power levels above 80 μW (−11 dBm) [13]. Several research groups have demonstrated such systems operating at RF input power of nearly 0 dBm [14–17]. Planar antennas and integrated circuits approaches have been employed to get conversion efficiencies in the range of 20–40% at such power levels.

In summary, the challenges one faces while harvesting low intensity RF signals are as follows: (1) Simple rectification is not feasible as the voltage level available is insufficient to overcome the forward bias threshold of schottky diodes, which is in the range

* Corresponding author. Tel.: +91 8022932967.
E-mail address: tvprabs@cedt.iisc.ernet.in (T.V. Prabhakar).

1434-8411/$ – see front matter © 2012 Elsevier GmbH. All rights reserved.
http://dx.doi.org/10.1016/j.aeue.2012.12.004

Table 1
A comparison of energy requirements for some commercially available low power radio chips operating in the 2.4 GHz ISM band.

Parameters	Jennic JN5148	TIMSP430 + CC2520
Active mode current at 16 MHz [mA]	6	4
Deep sleep current [nA]	100	1000
Transmission current [mA] @ Tx-power	15 mA @ 2.5 dBm	25.8 mA @ 0 dBm
Transmit frequency [GHz]	2.4	2.4
Wakeup time [ms]	1	0.3
Energy for a tx cycleof 4 ms [μJ]	183	300
Power supply voltage [V]	2.2–3.6	1.8–3.6

150–370 mV [18,19]. (2) Higher voltages at the output of rectifier are achieved with very high impedance loads. Therefore with practical loads the voltage available is insufficient. (3) Assuming that we use boost converters for step-up, there are two associated problems (a) they offer very low input resistance as load. And (b) their minimum input power requirement for continuous operation is higher than the power available. In order to address the above issues, we have recently proposed an accumulate-and-use topology to drive a commercial low power boost converter and secondary storage capacitors from the scavenged power from a tuned rectifier [20,21]. Energy efficient power gating and leakage management circuits are developed around a commercially available boost converter to enable this operation. Overall design philosophy of the system is described in Section 2. The design of the tuned rectifier, based on the identified requirements, is discussed in Section 3. The simulation and experimental characterization of the tuned rectifier circuits are discussed in Section 4. Results from ambient RF energy harvesting experiments using the developed harvesting system are included in Section 5. Using the circuit developed based on our approach, we were able to intermittently drive a low power radio requiring energy of 183 μJ for a single packet transmission utilizing incident RF power densities as low as 180 $\mu W/m^2$. Intermittent operation is necessary as the power required for the radio module during a packet transmission is 45 mW [23], which is much higher than the available input RF power.

2. Design philosophy of the harvesting system

The proposed harvesting system is designed to drive a low power wireless sensor node by accumulating energy from ambient RF radiations. In many countries where the regulations are stringent, the ambient power density available can be as low as $10\,nW/m^2$. However it is also reported that the power density (in at least at some hotspots if multiple cell phone towers are located in close vicinity) can be as high as $5\,mW/m^2$. For example, recently [15] reports an RF input of 130 μW (−9 dBm) from an antenna at a distance of 200 m from cellular towers with a receiving antenna gain of 9 dBi. This data is for a single carrier and single operator. Since in an urban setup we would typically have multiple carriers and multiple operators and with the minimum input power requirement of our system being 15 μW, we can cover a substantial fraction of urban areas. The energy requirement and other relevant characteristics for typical commercially available low power wireless radios are tabulated in Table 1. The energy consumption reported in Table 1 is of the order of 150–300 μJ for one transmission cycle (i.e., Sleep → Active → Transmission → Sleep). In addition, a supply voltage of 1.8–3.6 V at about 15–18 mA would be required to drive these systems. Since the power available would be insufficient to drive these continuously, accumulate and drive topology has been devised to overcome this. The design philosophy of the complete system is shown in Fig. 1. The system consists of a high gain antenna attached to a tuned rectifier. For a received

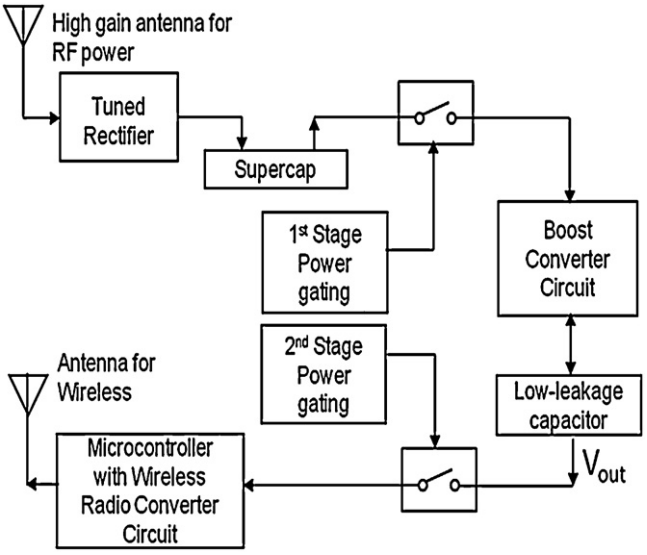

Fig. 1. Block diagram of the implementation.

RF power of 15 μW, the maximum DC voltage available at the output of this rectifier across the supercapacitor is about 400 mV. The 1st stage power gating circuit shown in Fig. 1 ensures that the boost converter does not load the supercapacitor. This phase is the accumulation phase. When supercapacitor is charged to the required voltage (170 mV in our case) the 1st stage power gating circuit generates a trigger pulse which enables the transfer of accumulated energy to the boost converter chip LTC3108 (Linear Technologies) which boosts the voltage and charges the output capacitor.

The tuned rectifier without the 1st stage power gating circuit cannot drive a commercial low power DC/DC boost converter as the in-line energy requirement will not be satisfied. Hence to store sufficient energy, a supercapacitor followed by an appropriate power gating circuit is used at the output of the rectifying circuit. The total energy transferred from the supercapacitor to the output load can be given as:

$$E_{out} = ((E_{supercap} - E_{startup}) \times n_{boost}) \quad (1)$$

where $E_{startup}$ is the energy required to start the operation of the boost converter, i.e., for charging various internal and external capacitors required to power up. To maximize the overall efficiency, the startup component which is wasted every cycle of intermittent operation should be made insignificant. This can be achieved by increasing either the voltage across the supercapacitor or its capacitance value. However, increasing the voltage across the supercapacitor would increase the internal leakage in the supercapacitor, affecting the efficiency of the rectifying section. Furthermore due to practical limits of achievable Q, tuned rectifier can generate only a few hundred millivolts at the intended power level of 15 μW. Also since the efficiency of the boost converter varies with the input voltage, the supercapacitor operating voltage range is decided such that it maximizes the combined efficiency of RF–DC and the boost converter stage. The instantaneous efficiency of RF–DC section is defined as the ratio of rate of change of energy stored in supercapacitor and the input power P_{in}:

$$\eta_{inst} = \frac{1}{P_{in}} \frac{d}{dt} \frac{CV^2}{2} = \frac{1}{P_{in}} C \frac{dV}{dt} \quad (2)$$

The instantaneous output voltage of the tuned rectifier may be differentiated to obtain the instantaneous efficiencies for different incident power levels. A graph of the same is plotted in Fig. 8 and it is clear that for a given input power, the efficiency peaks when the rectifier output is kept at a particular voltage. In an intermittent

Please cite this article in press as: Singh G, et al. A tuned rectifier for RF energy harvesting from ambient radiations. Int J Electron Commun (AEÜ) (2013), http://dx.doi.org/10.1016/j.aeue.2012.12.004

operation scenario, one is interested in the efficiency over a voltage range. Thus, one can define period efficiency as the overall efficiency during an interval of charging from voltage V_1 to V_2 at a particular input power level. It is the ratio of energy stored in time ΔT in the supercapacitor to the energy supplied at the input during the same period:

$$\eta_{period} = \frac{CV_2^2 - V_1^2}{2P_{in}\Delta T} \quad (3)$$

The period efficiency can be related to the instantaneous efficiency η_{inst} V as

$$\eta_{period} = \frac{V_2^2 - V_1^2}{2\int_{V_1}^{V_2} V(1/\eta_{inst(V)})dv} \quad (4)$$

In the special case where η_{inst} (v) is fairly constant in the voltage range V_1–V_2 (so that it can be taken outside the integration) η_{period} reduces to η_{inst}. Therefore period efficiency can be theoretically maximized (=instantaneous efficiency) by choosing an operating voltage range (V_1–V_2) very close to the peak of instantaneous efficiency curve. In our implementation we have used LTC3108 as the boost converter. The input voltage vs. efficiency of this device [11] shows that the maximum efficiency is achieved when a 1:20 fly back transformer is used. For this transformer, it is possible for the input of the boost converter to start from 100 mV and the efficiency is claimed to be 60% for continuous operation. The efficiency decreases linearly to 50% as the input voltage is increased to 150 mV and reduces to 20% for voltage higher than 200 mV. Therefore, to maximize the combined efficiency of the RF–DC stage plus boost converter at various input power levels and also keeping in view the energy requirements of the power management circuitry and boost converter (ensuring $E_{supercap} \gg E_{startup}$) a supercapacitor value of 33 mF and voltage range of V_1 = 120 mV and V_2 = 170 mV has been chosen. How the efficiency of RF–DC section is maximized for this voltage range is discussed in Section 4. The 1st stage power gating circuit ensures that the voltage across supercapacitor is within V_1 and V_2. Since the maximum voltage across the supercapacitor in our case is 170 mV (much less than the rated voltage of the supercapacitor used −5.5 V [24]) the leakage power will be extremely small [25,26]. This is in contrast to most reported systems which typically have a supercapacitor connected at higher voltage levels [7]. The higher voltages in our case obtained at the output of boost converter are stored in low-leakage ceramic capacitor. When the voltage reaches to the programmed value (between 2.2 V and 4.5 V) the 2nd stage of power gating circuit, shown in Fig. 1, connects the load to this storage capacitor. In our demonstration setup, the accumulated energy is used to drive a low power sensor node (Jennic JN 5148) that senses the ambient temperature and transmits the data to a base station. There is no external power supply for any of the components of the circuit shown here, and it can operate continuously as long as the minimum RF power of 15 μW is available at the input of the tuned rectifier. This corresponds to an ambient radiation intensity of 180 μW/m^2, assuming receiving antenna gain of 10 dB. Very recently, a patent application based on a similar two-stage topology for RF energy has been filed [22] although the implementation details or performance parameters are not readily available.

3. Design of the tuned rectifier

In this configuration an antenna with an input impedance of 50 Ω is used with the rectifier to harvest the radiations. If the RF power available from the antenna is directly fed into an ideal half wave rectifier circuit, a peak DC voltage level of only about 30 mV can be obtained for an RF power of 15 μW at the rectifier input. This would be insufficient to operate any active device. Hence an

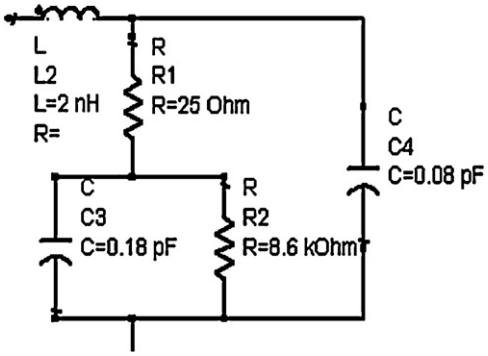

Fig. 2. Equivalent circuit of HSMS285x.

L-section impedance matching circuit is used between the antenna and the rectifying diode. The quality factor of this matching section enhances the voltage level. However, the realizable Q would restrict the output voltage to several hundreds of mV. The rectifier circuit has been designed using RF schottky diode AVAGO HSMS285C due to its very low junction capacitance (0.18 pF), and barrier voltage (150 mV). This diode also has a high voltage sensitivity of 40 mV/μW in a detector circuit. The impedance matching section for the rectifier circuit is designed and simulated using Agilent ADS 2009. The equivalent circuit of this diode is shown in Fig. 2. The impedance of the diode is mainly capacitive (junction C3 and package capacitance C4), with a large junction resistance (R2) in parallel. In addition there is a small resistance of 25Ω in series (package resistance R1). The equivalent circuit model is obtained based on the insertion loss within the GSM frequency band (930–960 MHz) for an incident RF power of −20 dBm [18]. The matching circuit is designed using ADS assuming that the tuned rectifier is driving the supercapacitor (not shown) at port 2 of Fig. 3. It may be noted that this port impedance load condition is rather non-conventional from RF circuit design point of view. Typically rectifier circuits are characterized with high resistive impedance at the output (DC) port to demonstrate large voltages. The circuit parameters are optimized for a center frequency of 945 MHz. In the circuit shown in Fig. 3, TL3 is a 50Ω transmission line to connect RF input port and the output is taken across the capacitor C2. The capacitor C2 has to be placed very close to the rectifying diode, as it acts like a RF ground and ensures that tuning circuit is not affected by any parasitic inductances either from the track or load (supercapacitor). The inductor L1 is connected in series to change the input reactance of the diode to a point directly below the center of the Smith Chart. The additional shunt inductance provided by the transmission line TL1 is used to match the circuit at its input to the antenna impedance of 50 Ω. This transmission line is designed to have a shunt reactance of j48Ω in this case. In the circuit, TL2 is a very short transmission line segment used to mount the leads of the diode and the inductor. The physical dimensions of the

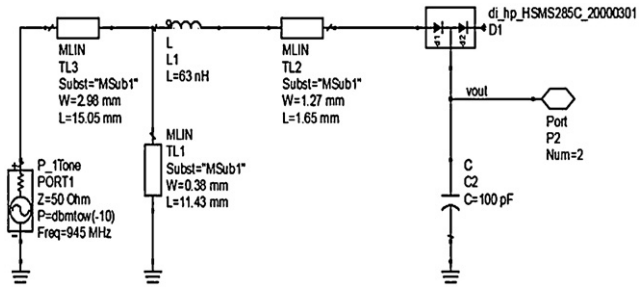

Fig. 3. Tuned rectifier.

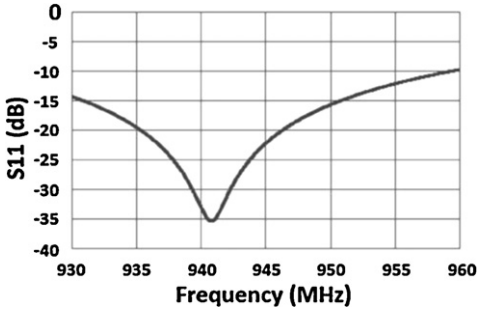

Fig. 4. Simulated S11 characteristics of the tuned rectifier.

transmission lines and values for components depend on the substrate (FR-4) used.

The impedance matching has been done using reactive elements. This reduces the input bandwidth and hence surface-mount components for this circuit are carefully chosen to have high accuracy and low tolerance. On the other hand, the reactive matching approach improved the sensitivity of the overall circuit. The quality factor of this circuit provides a passive amplification of the input signal. However the intention was not to amplify it beyond a few hundred millivolts before storing in the super capacitor. Higher voltage amplification is possible with doublers and cascaded multipliers [9], but this is expected to be unnecessary from the efficiency point of view as explained previously in Section 2. The performance of the tuned rectifier output is evaluated by investigating the RF characteristics (S11) at its input as well as for RF–DC energy conversion characteristics under various conditions. Fig. 4 shows the simulated S11 characteristics of this circuit, with an ideal capacitor of 100 pF as the load. We assumed this load instead of 33 mF for two reasons: (a) Reliable ADS library models for supercapacitors are not readily available and (b) Simulation time to reach the peak output for 100 pF load is significantly lower compared to 33 mF. Fig. 5 shows the simulation results for the output of the rectifier circuit for several values of input power at 945 MHz.

4. Characterization of the tuned rectifier

In this section the characterization and results for the tuned rectifier of the harvesting system are discussed. As the performance of the circuit depends on the load conditions two separate cases are considered for the evaluation of the rectifier. The synthesized sweeper of a vector network analyzer is used for the characterization of this circuit to directly supply the input at the desired frequency and power level.

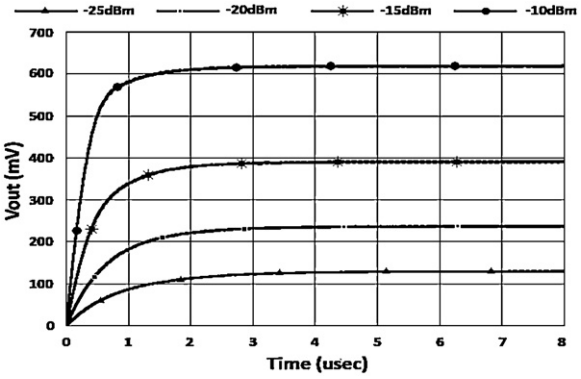

Fig. 5. Simulation results for the tuned rectifier for various input power levels at 945 MHz and a load impedance of 100 pF.

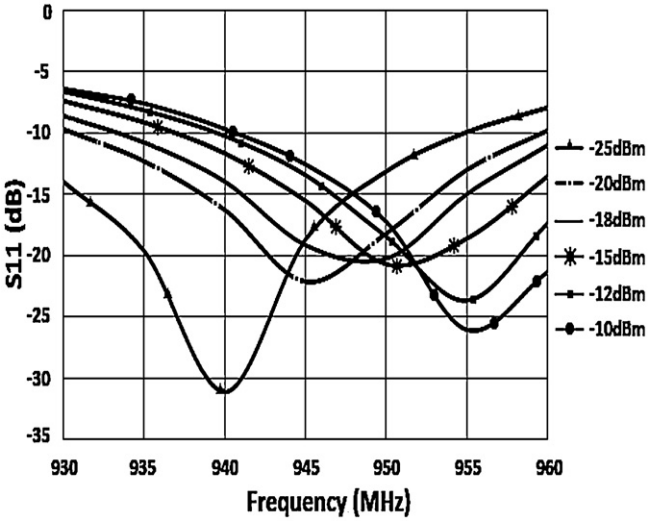

Fig. 6. Measured S11 characteristics of the tuned rectifier.

Table 2
Comparison of simulated and measured steady state output of the rectifier circuit at 945 MHz when terminated with 100 pF capacitor.

Input power, dBm	Steady state voltage	
	Simulated	Experimental
−25	140	132
−20	240	300
−15	400	580
−10	620	1016

4.1. Characterization under standard load conditions

An extended experimental characterization of the tuned rectifier is done by varying frequency and the input power. These measurements are performed without supercapacitors at the output of the tuned rectifier. Fig. 6 shows the measured S11 characteristics of this circuit at the RF input port with the output terminated by 100 pF capacitor for various input power. It is seen that the impedance matching shifts towards higher frequency as the power levels are increased. This is due to the dependence of the junction capacitance and the diode resistance on the input power. However, the return loss is better than −10 dB at the frequency of 945 MHz at all power levels.

The comparison of the peak voltage obtained from simulation (Fig. 5) and measurements by varying the input power at a fixed frequency of 945 MHz is shown in Table 2. The design parameters mentioned for HSMS285C diode in the datasheet, using which the matching circuit was designed, are for power levels less than −20 dBm. The practical results at higher power levels are therefore different. The measured results in Table 3 confirm that the steady state output voltage from the rectifier depends on the RF input power and is fairly independent of frequency within the band of interest.

Table 3
Measured steady state output of the tuned rectifier for different RF input power levels at various frequencies when the circuit is terminated with 100 pF capacitor.

P_{in}, MHz	DC output (mV) at different input power				
	−10	−13	−16	−20	−25
930	917	664	469	281	131
945	1016	736	515	300	132
955	1038	747	513	289	122
960	1032	736	499	276	114

Please cite this article in press as: Singh G, et al. A tuned rectifier for RF energy harvesting from ambient radiations. Int J Electron Commun (AEÜ) (2013), http://dx.doi.org/10.1016/j.aeue.2012.12.004

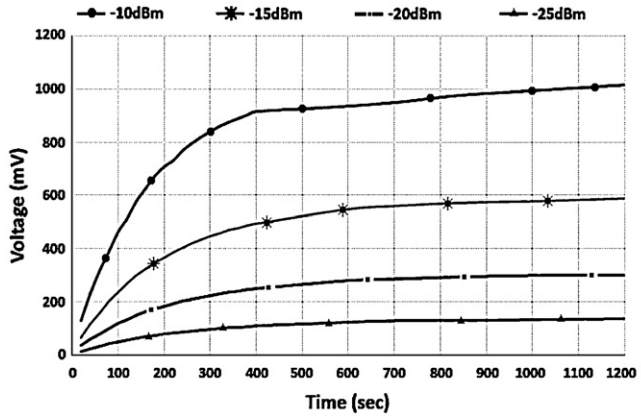

Fig. 7. Charging of a 33 mF supercapacitor at 945 MHz for different power levels vs. time.

4.2. Characterization with supercapacitor connected

Based on the analysis discussed in Section 2, the rectifier is characterized with the intended supercapacitor load of 33 mF. Voltage across the supercapacitor is measured for duration of 20 min for each RF input power level. Plot of which is shown in Fig. 7. It may be recalled that the instantaneous efficiency is the ratio of rate of energy stored in supercapacitor to the input power as given in Eq. (2). We obtain dV/dt from Fig. 7 for different input power levels, to plot the instantaneous efficiency for those different power levels as a function of output voltage as shown in Fig. 8. From Fig. 8 we can see that the efficiency of RF–DC stage is maximum when the supercapacitor voltage is around 150 mV at −20 dBm input power. As discussed in Section 2, to ensure the combined efficiency of RF–DC stage and the boost converter is maximized, the operating voltage range across the supercapacitor has been fixed between 120 and 170 mV.

5. Wireless transmission using harvested energy

The tuned rectifier described in the previous sections is used to power up a commercial low power DC/DC boost converter along with necessary power gating and leakage management circuits to demonstrate wireless transmission using the harvested energy. Fig. 9 shows the photograph of the prototype board developed for this purpose. The low power wireless module (Jennic JN5148) is integrated in this board. The radio module is programmed to send

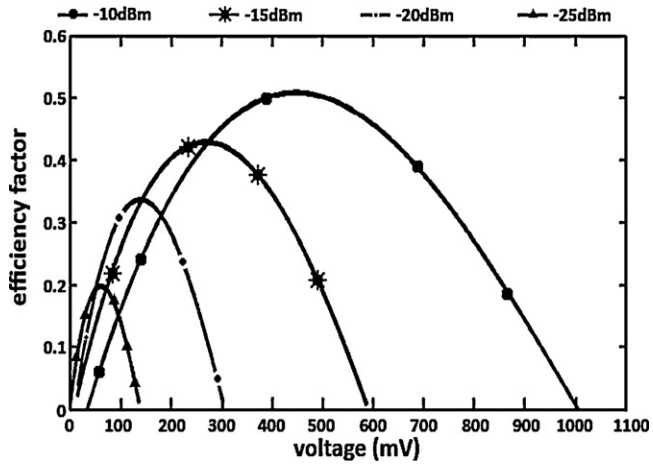

Fig. 8. RF–DC conversion efficiency as a function of supercapacitor voltage (Fig. 7) for different RF input power levels @ 945 MHz.

Fig. 9. The fabricated harvester board. The RF power is received by an external antenna connected though SMA port. The antenna shown is for the wireless radio.

Table 4
Measured steady state output of the tuned rectifier for different RF input power levels at various frequencies when the circuit is terminated with 100 pF capacitor.

Input RF power (dBm)	Packet transmission interval (mm:ss)
−10	1:25
−11	1:55
−12	2:20
−13	2:55
−15	7:20
−16	12:21
−17	21
−18	66

an 8 byte data packet containing the ambient temperature data when turned ON. Since the harvested energy available would differ based on ambient conditions, the rate of transmission is used here as a measure of the harvested energy. Another wireless module connected to a laptop acts as a receiver. This integrated board is evaluated in two stages: (a) first by feeding this with direct RF power from network analyser and (b) by providing radiated power through an antenna. This experiment was carried out inside an anechoic chamber. In the first experiment, the board is characterized by directly feeding CW power at different power levels. We have evaluated the rate of transmission at various input RF power levels. The measured transmission frequency vs. input RF power at 945 MHz has been shown in Table 4. The setup for the 2nd part of the experiment is shown in Fig. 10. The wireless module, tuned rectifier and the rest of power management circuits and boost converter are integrated as shown in Fig. 9. A high gain biquad antenna is used to transmit the CW RF power (10 dBm) from the network

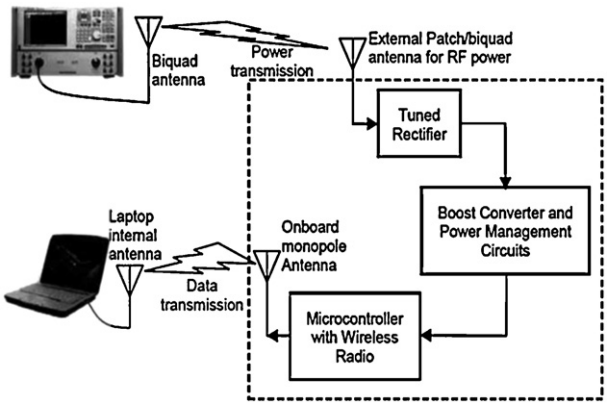

Fig. 10. Schematic of the experimental setup to demonstrate wireless transmission using scavenged RF power.

Table 5
Measured steady state output of the tuned rectifier for different RF input power levels at various frequencies when the circuit is terminated with 100 pF capacitor.

Distance from transmitter [m]	1.5	2	2.5	3
Power received by dipole antenna [dBm]	−20.5	−22.1	−23.9	−25.2
Calculated power density [$\mu W/m^2$]	780	550	350	300
Power received by biquad antenna [dBm]	−11.8	−13.2	−14.9	−15.9
Transmit interval [mm:ss]	02:20	03:25	7:10	10:33

analyzer. The biquad antenna is designed based on [27] and has a 10 dB return loss band ranging from 920 MHz to 1000 MHz. This antenna has a gain of 10.5 dBi at 945 MHz. The synthesized sweeper of the network analyzer is used as an RF power source. Another biquad antenna is used to receive the RF power at 945 MHz. Power received by a 2 dB dipole antenna is used as a reference to calculate the power density at the location of the receiving unit by connecting the antenna to a spectrum analyzer. Since the power management circuit turns on the low power wireless module at an interval based on the incident RF energy, the transmission interval has been found for different power densities. Table 5 shows the performance of the integrated board in this situation. These experiments demonstrate that energy can be harvested from ambient radiations as low as $180\mu W/m^2$ which is present in many urban locations and can be harvested using a 10.5 dBi gain antenna. It is also possible to energize remote wireless sensor network nodes in a controlled environment using conveniently located radiators. It is believed that this approach of harvesting energy can benefit the ubiquitous utilization of wireless sensors [28]. Wearable or buried sensors can be powered up using electromagnetic energy and data collected by this approach [14,29].

6. Summary and conclusions

Electromagnetic energy available from sources like cellular network towers, mobile phones, WIFI network, etc. has been found to be substantial in urban areas, with the power density ranging up to 10 mW/m^2 [8]. A unique two-stage accumulate-and-drive topology for such a harvesting system to energize a wireless sensor node is demonstrated. The RF design of a tuned rectifier to meet the requirements for this harvesting system is discussed in this paper. In order to quantify the performance in a calibrated environment, measurements in an anechoic chamber are presented. The results indicate that the designed tuned rectifier has a peak efficiency range of 32–52% as the input power varies from 10 μW to 100 μW. With newer radios operating at 10 nJ/bit becoming a reality, harvested RF energy would be sufficient for such devices and therefore holds the key for energy reuse for wireless sensing applications.

References

[1] Brown WC. The history of power transmission by radio waves. IEEE Trans Microw Theory Tech 1984;MTT-32:1230–42.
[2] http://seattle.intel-research.net/pubs/WISP-WARP.pdf
[3] Epp LW, Khan AR, Smith HK, Smith RP. A compact dual-polarized 8.51 GHz rectenna for high voltage (50 V) actuator applications. IEEE Trans Microw Theory Tech 2000;48:111–20.
[4] McSpadden JO, Mankins JC. Space solar power programs and microwave wireless power transmission technology. IEEE Microw Mag 2002;3(December 4):44–57.
[5] McSpadden JO, Fan L, Chang K. Design and experiments of a high-conversion-efficiency 5.8-GHz rectenna. IEEE Trans Microw Theory Tech 1998;46(December (12 Pt 1)):2053–60.
[6] McSpadden JO, Fan L, Chang K. Design and experiments of a high-conversion-efficiency 5.8-GHz rectenna. IEEE Trans Microw Theory Tech 1998;46:2053–60.
[7] Bharj SS, Camisa R, Grober S, Wozniak F, Pendleton E. High efficiency C-band 1000 element rectenna array for microwave powered applications. In: IEEE MTT-S Int Microwave Sympos Dig. 1992. p. 301–3.
[8] http://www.ee.iitb.ac.in/ mwave/GK-cell-tower-rad-report-DOT-Dec2010.pdf
[9] Le T, Mayaram K, Fiez T. Efficient far-field radio frequency energy harvesting for passively powered sensor networks. IEEE J Solid-St Circ 2008;43(May (5)).
[10] Olgun U, Chen C-C, Volakis JL. Investigation of rectenna array configurations for enhanced RF power harvesting. IEEE Antenn Wireless Propag Lett 2011;10:262–5.
[11] www.cds.linear.com/docs/Datasheet/3108fa
[12] http://ww1.microchip.com/downloads/en/DeviceDoc/22234B.pdf
[13] http://www.powercastco.com/PDF/P2110-datasheet.pdf
[14] Nasotti D, Contanzo A, Adami S. Design and realization of a wearable multi-frequency RF energy harvesting system. In: Proceedings of the 5th European conference on antennas and propagation (EUCAP). 2011. p. 517–20.
[15] Arrawatia M, Baghini MS, Kumar G. RF energy harvesting system from cell towers in 900 MHz band. In: National conference on communications. 2011.
[16] Paing T, Falkenstein E, Zane R, Popovic Z. Custom IC for ultra-low power RF energy harvesting. In: Twenty-fourth annual IEEE applied power electronics conference and exposition. 2009. p. 1239–45.
[17] Dolgov A, Zane R, Popovic Z. Power management system for online low power RF energy harvesting optimization. IEEE Trans Circ Syst I 2010;57(July (7)):1802–11.
[18] www.avagotech.com/docs/AV02-1377EN
[19] http://www.vishay.com/docs/82392/bas58102.pdf
[20] Singh G, Ponnaganti R.RF energy harvesting IETE conference on RF and wireless (Icon RFW-11). 2011.
[21] Singh G, Ponnaganti R. Ambient RF energy harvesting and monitoring. M.Tech. Dissertation. Centre For Electronics Design and Technology, Faculty of Engineering, Indian Institute of Science, Bangalore; June 2011.
[22] Tinaphong PP. Method and apparatus for harvesting energy. US Patent Application #20110175461. Audiovox Corporation, Hauppauge, NY; July 21, 2011.
[23] http://www.jennic.com/files/product_briefs/JN-DS-JN5148-1v6.pdf
[24] http://www.avx.com/docs/catalogs/bestcap.pdf, part no.: BZ055A333Z_B.
[25] Renner C, Jessen J, Turau V. Lifetime prediction for supercapacitor-powered wireless sensor nodes. In: Proceedings of the 8th GI/ITG KuVSFachgesprch 'DrahtloseSensornetze'. 2009. p. 55–8.
[26] Mahlknecht S, Roetzer M. Energy supply considerations for self-sustaining wireless sensor networks, Energy supply considerations for self-sustaining wireless sensor networks.
[27] Straw RD, editor. In: ARRL antenna book. Newington, CT: ARRL; 2007 [chapter 12].
[28] Akyildiz IF, Su W, Sankarasubramaniam Y, Cayirci E. Wireless sensor networks: a survey. Comput Netw 2002;38(March (4)):393–422.
[29] Mascareas D, Flynn E, Farrar C, Park G, Todd M. A mobile host approach for wireless powering and interrogation of structural health monitoring sensor networks. IEEE Sens J 2009;December 9(12):1719–26.

Please cite this article in press as: Singh G, et al. A tuned rectifier for RF energy harvesting from ambient radiations. Int J Electron Commun (AEÜ) (2013), http://dx.doi.org/10.1016/j.aeue.2012.12.004